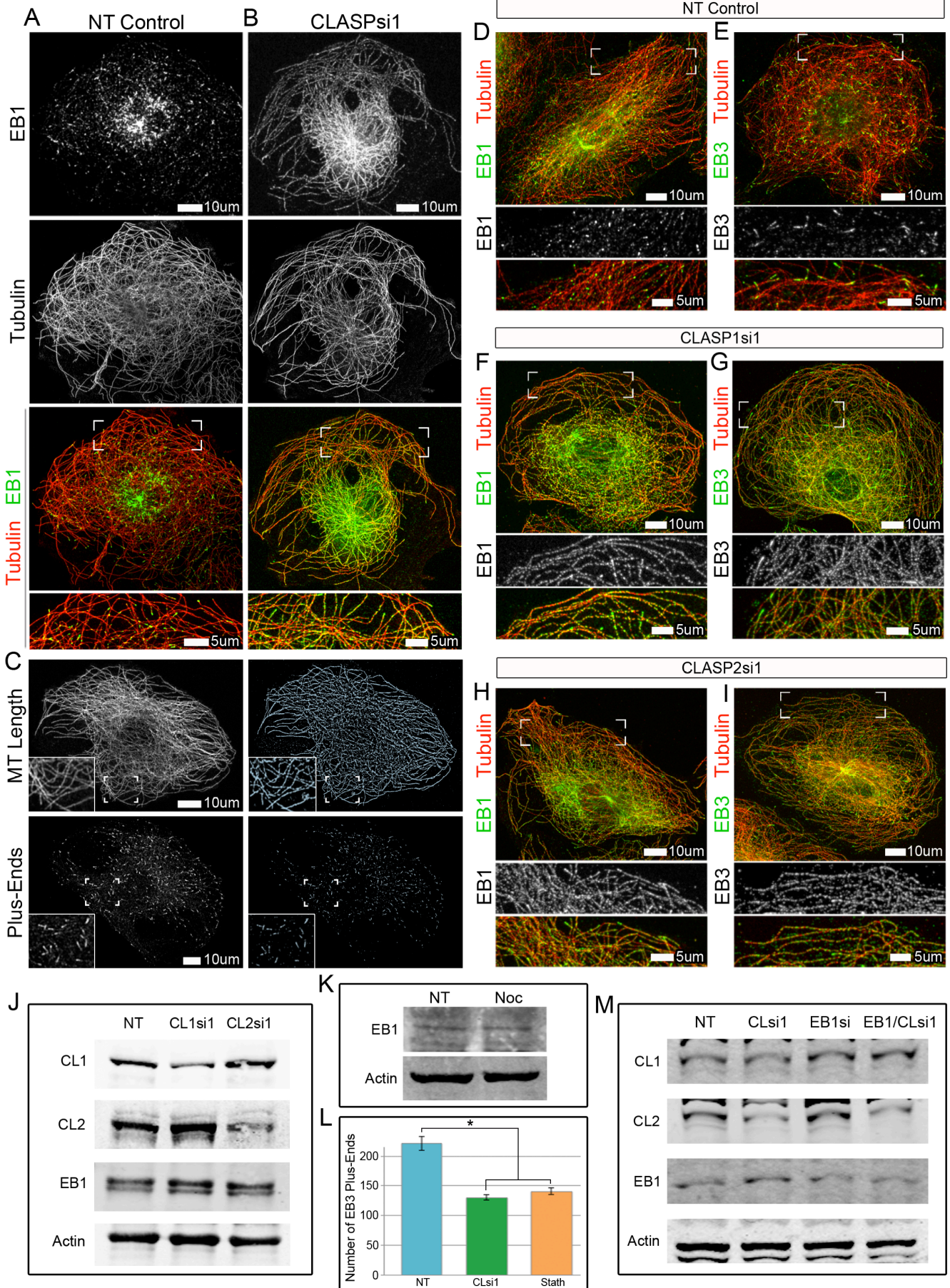


# Supplemental Information

## Supplemental Figures



## CLASPs promote exclusive EB plus-end localization

**Figure S1.** CLASPs 1 and 2 redundantly regulate EB localization at microtubules, related to Figure 1.

(**A-B**) Immunofluorescence images of A7r5 cells stained for  $\alpha$ -tubulin (red) and EB1 (green). (**A**) EB3 localizes to MT plus-ends in NT control cells. (**B**) EB3 extensively coats the MT lattice, in addition to its normal plus-end localization, in CLASP-depleted cells. (**C**) Examples of Imaris MT fitting for MT length quantification (**N** in Figure 1) and plus-end fitting for number of EB3 plus-end quantification in (**L**). (**D-I**) Immunofluorescence images of A7r5 cells stained for  $\alpha$ -tubulin (red) and either EB1 or EB3 (green). (**D,E**) EBs localizes to MT plus-ends in NT control cells. (**F,G**) EBs partially coat the MT lattice, in addition to their normal plus-end localization, in CLASP1-depleted cells. (**H,I**) Similarly, EBs partially coat the MT lattice, in addition to their normal plus-end localization, in CLASP2-depleted cells. (**A-I**) Merge zoomed region is indicated by boxed corners in Merge. White box=scale bar. (**J**) Western blot of A7r5 whole cell lysate showing specificity of siRNAs against CLASP1 and CLASP2. EB1 protein levels did not change in cells depleted individually of either CLASP1 or CLASP2. (**K**) Western blot of A7r5 whole cell lysate showing no change in EB1 protein levels upon Nocodazole treatment when compared to NT control. (**L**) Average number of EB3 plus-ends in NT control, CLASP-depletion, and GFP-Stathmin expression. Based on data similar to (**A,B,D**) in Figure 1. Values are normalized means  $\pm$  S.E.M. (n=15, 3 independent experiments). Student's unpaired two-tailed t-test. Asterisks,  $p < 0.05$ . (**M**) Western blot of RPE whole cell lysate showing both CLASP1 and CLASP2 protein levels upon CLASP-depletion, EB1 protein levels upon EB1 partial depletion, and CLASPs and EB1 protein levels upon double depletion, when compared to NT control. (**J,K,M**) Actin was used as a loading control.



## CLASPs promote exclusive EB plus-end localization

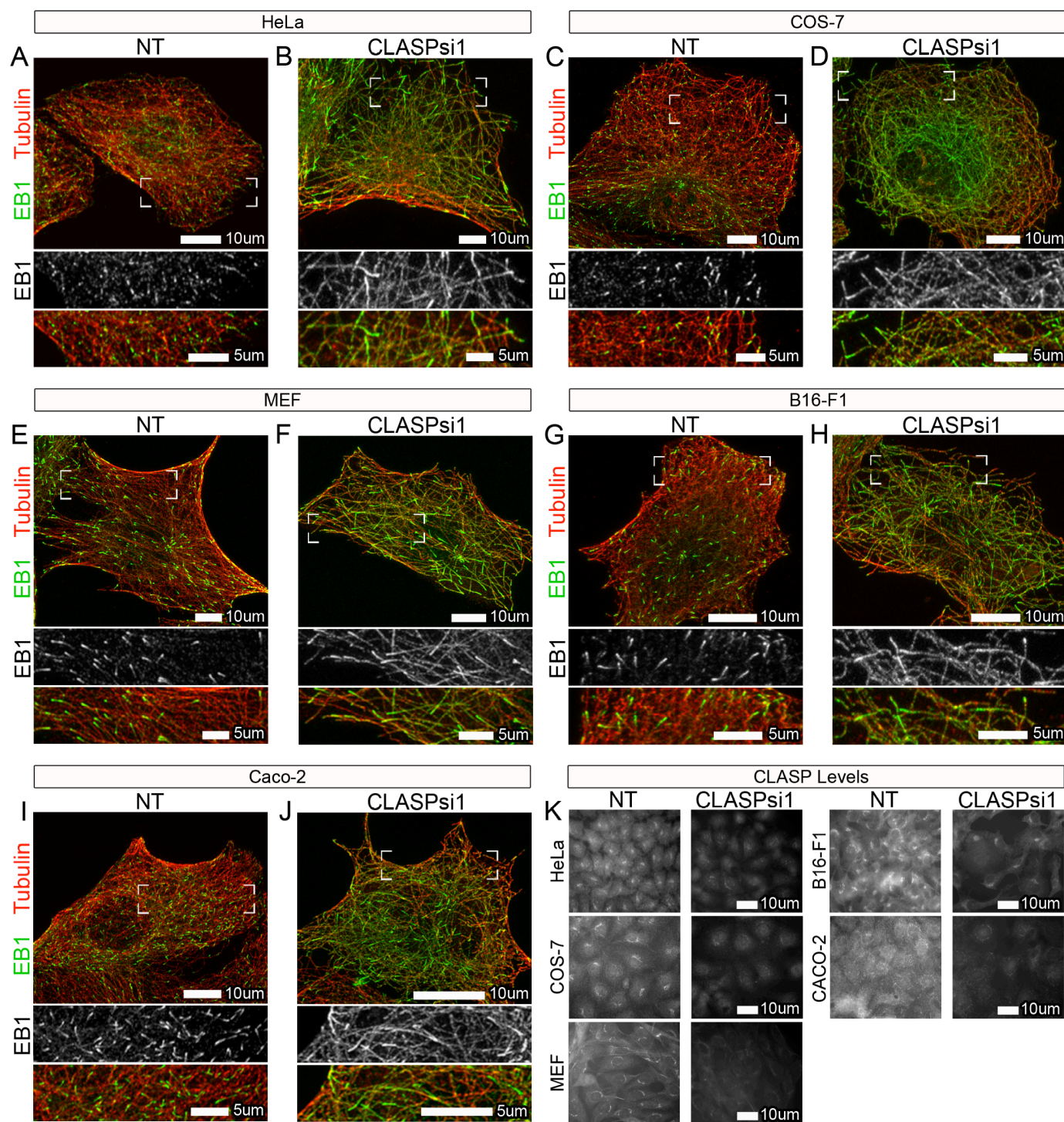


**Figure S2.** Altered EB localization in CLASP-depleted cells is not cell type specific, related to Figure 1.

(A-J) Immunofluorescence images of various cell types stained for  $\alpha$ -tubulin (red) and EB1 (green). EB1 extensively relocalizes to the MT lattice, in addition to plus-ends, in CLASP-depleted cells (B,D,F,H,J), when compared to NT control (A,C,E,G,I). (A,B) HeLa. (C,D) COS-7. (E,F) MEF. (G,H) B16-F1. (I,J) Caco-2. (K) Representative widefield images showing reduced pan-CLASP levels upon CLASP-depletion in each cell type. (A-K) White box=scale bar.



## CLASPs promote exclusive EB plus-end localization

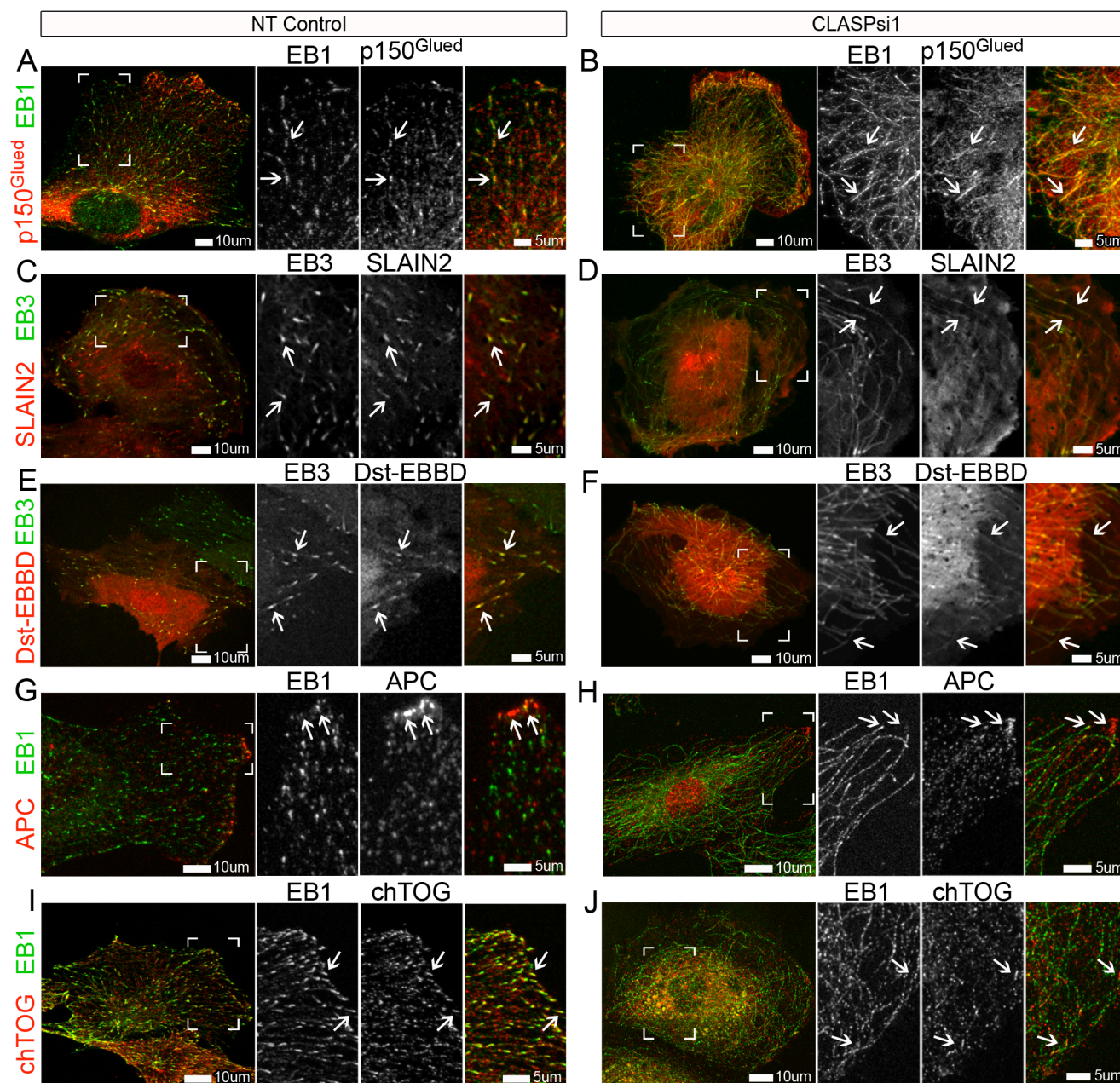


**Figure S3.** +TIP proteins relocalize with EBs in CLASP-depleted cells, related to Figure 2.

(A-D,I,J) Immunofluorescence images of RPE cells stained for EB1 or EB3 (green) and proteins representative of the major +TIP families (red). (E-H) Single confocal slice of A7r5 cells expressing tdTomato-EB3 (green) and proteins representative of the major +TIP families (red). (A) EB3 and p150<sup>Glued</sup> (CAP-Gly family) both localize to MT plus-ends in a NT control cell. (B) In addition to EB3, p150<sup>Glued</sup> also relocalizes to the MT lattice in a CLASP-depleted cell, as was seen for CLIP-170. (C) tdTomato-EB3 and GFP-SLAIN2 (SxIP family) both localize to MT plus-ends in a NT control cell. (D) GFP-SLAIN2 relocalizes with tdTomato-EB3 to the MT lattice in a CLASP-depleted cell. (E) tdTomato-EB3 and the minimal EB-Binding Domain of Dystonin (GFP-Dst-EBBD, SxIP family) both localize to MT plus-ends in a NT control cell. (F) In addition to tdTomato-EB3, GFP-Dst-EBBD also relocalizes to the MT lattice in a CLASP-depleted



## CLASPs promote exclusive EB plus-end localization

cell. **(G)** EB1 localizes to MT plus-ends, while APC (SxIP family) localizes to patches at the cell periphery as well as occasional MT plus-ends in a NT control cell. **(H)** EB1 relocates to the MT lattice in a CLASP-depleted cell, while APC localization upon CLASP-depletion does not differ from NT control. **(E)** EB1 and chTOG (EB-independent) both localize to MT plus-ends in a NT control cell. **(F)** EB1 relocates to the MT lattice in a CLASP-depleted cell, while chTOG localization upon CLASP-depletion does not differ from NT control. **(A-J)** Merge zoomed region is indicated by boxed corners in Merge. White arrows indicate examples of EB/+TIP characteristic localization or lattice relocation respectively. White box=scale bar.

## CLASPs promote exclusive EB plus-end localization

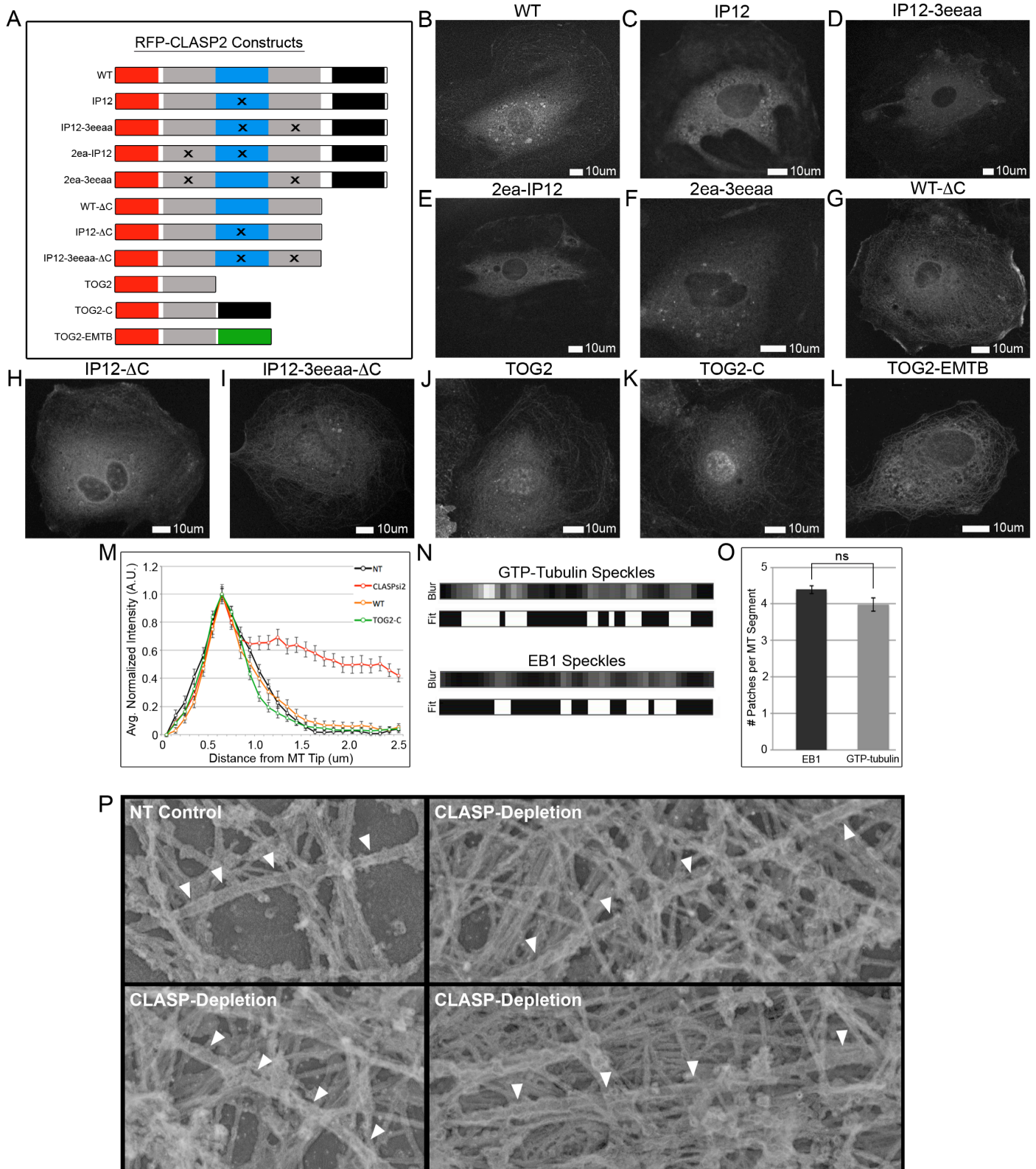


**Figure S4.** Localization of CLASP mutant constructs in A7r5 cells, related to Figure 3 and Figure 4.

(A) Schematic representation of RFP-CLASP2 and mutant CLASP2 rescue constructs. Red=RFP tag, grey=TOG-containing MT binding domains (TOG2 and TOG3), blue=EB-binding region (basic/SxIP), black=C-Terminus, and green=MT-binding domain of Ensconsin (EMTB). (B-L) Immunofluorescence.



## CLASPs promote exclusive EB plus-end localization

Expression of RFP-tagged CLASP2 constructs in control A7r5 cells (grey). **(B)** WT CLASP2 localizes to MT plus-ends. **(C-F)** CLASP2 mutant constructs IP12 **(C)**, IP12-3eeaa **(D)**, 2ea-IP12 **(E)**, and 2ea-3eeaa **(F)** display low levels of MT-binding with a diffuse cytoplasmic localization. **(G-L)** Short CLASP2 constructs lacking the C-terminal region, WT- $\Delta$ C **(G)**, IP12- $\Delta$ C **(H)**, IP12-3eeaa- $\Delta$ C **(I)**, TOG2 **(J)**, TOG2-C **(K)**, and TOG2-EMTB **(L)**, displayed enhanced MT localization. **(J-L)** The shortest TOG2-containing CLASP2 constructs showed low levels of MT bundling, which corresponded to the level of construct expression. **(B-L)** White box=scale bar. **(M)** Line scan analysis quantifying rescue of normal CLIP-170 plus-end localization in CLASP-depleted cells expressing the minimal TOG2-C rescue construct. Line scan values are normalized mean intensities  $\pm$  S.E.M. (n=50, 2 independent experiments). **(N)** Binary fit of GTP-tubulin and EB1 speckles along MT lattice after initial blur step. **(O)** Number of EB1 and GTP-tubulin patches per MT segment. Based on data similar to **(N)**. Student's unpaired two-tailed t-test. Asterisks,  $p < 0.05$ . **(P)** Platinum replica EM showing lack of MT bundling in CLASP-depleted cells when compared to NT control. White arrowhead indicates MT.

## Supplemental Experimental Procedures

### *Transfection, lentiviral infection, and stable lines*

For transient transfection of plasmid DNA, Fugene6 (Roche) was used and for siRNA oligonucleotide transfection, HiPerFect (Qiagen) was used according to manufacturer protocols. RFP-CLASP2 stable lines were generated using lentiviral constructs. For viral infection, supernatant containing lentiviral particles was collected from HEK293T cells transfected with lentiviral expression vectors and second generation packaging constructs (Invitrogen). A7r5 cells were infected with supernatant containing lentiviral particles with 8mg/ml polybrene overnight.

### *siRNA Depletions and Drug Treatments*

Two different combinations of mixed small interfering RNA (siRNA) oligonucleotides against CLASP1 and CLASP2 were transfected into cells. Combination #1 (Dharmacon): CLASP1 siRNA targeted sequence 5'-GGATGATTTACAAGACTGG-3'; CLASP2 siRNA targeted sequence 5'-GACATACATGGGTCTTAGA-3', Combination #2 (custom design, Sigma): CLASP1 siRNA targeted sequence 5'-GCCATTATGCCAACTATCT-3'; CLASP2 siRNA targeted sequence 5'-GTTTCAGAAAGCCCTTGATG-3'. In the text and figures, CLASPsi1/CLsi1=siRNA combination #1 and CLASPsi2/CLsi2=siRNA combination #2. Combination #2 was used for CLASP rescue experiments. Non-targeting siRNA (Dharmacon) was used as a control. Experiments were conducted 72 hours after siRNA transfection, as, at this time, minimal protein levels were detected by western blot analysis.

## CLASPs promote exclusive EB plus-end localization

A small interfering RNA (siRNA) oligonucleotide against EB1 (custom design, Sigma) was transfected into cells: 5'-GACUAUGACCCUGUGGCUG-[dT]-[dT] 3'. Experiments were conducted 48 hours after siRNA transfection, as minimal protein levels were detected by western blot analysis at this time.

For MT depolymerization, cells were briefly treated with 1.5µg/mL nocodazole for 5-10min to decrease MT numbers to resemble those of CLASP-depleted cells. Alternatively, GFP-Stathmin was transfected by nucleofection according to the manufacturer's protocol (Lonza, program X-001) and expressed at low levels for 72 hours (same time as CLASPs siRNA treatment) to decrease MT numbers.

### *Expression Constructs*

A novel mEmerald-EB3 construct was designed with an mEmerald tag on the N-terminus of EB3 and a 20 amino acid linker between mEmerald and EB3. The Emerald sequence is WT GFP with the following mutations: F64L/S65T/S72A/N149K/M153T/I167T/A206K. The Linker sequence between mEmerald and EB3 is composed of the amino acids: SGLRSGSGGGSASGGSGSGG. The EB3 sequence was cloned into an mEmerald C1 cloning vector (Clontech-style where mEmerald replaces EGFP) after amplification with the following primers:

Forward:GCCGTCAATGTGTACTCCACATCTGTGACCTCCGGACTCAGATCTGGCAGCGGTGGAGGCAGC  
GCATCCGGCGGAAGCGGAAGCGGGGA

Reverse:GAGATTGAAGAGCATCAACAAGAAGACCAGGACGAGTACTAAGGATCCACCGGATCTAG

The mEmerald-C1 cloning vector and EB3 PCR reaction were both cut with BamHI and BglII restriction enzymes, gel purified, and ligated to construct the final targeting vector.

EB3-GFP was a gift from J. Victor Small (Austrian Academy of Sciences, Austria). EB3-N-LZ-GFP, an artificial dimer of the EB3 CH MT binding domain which lacks most of the linker region, was a gift from Anna Akhmanova and has been previously described (Komarova et al., 2009); GFP-SLAIN2 was also a gift from Anna Akhmanova (Utrecht University, Netherlands). GFP-Stathmin was kindly provided by Martin Gullberg (Umea University, Sweden). GFP-Dst-EBBD, the minimal EB-binding domain of mouse Dystonin, was cloned as an XhoI-MfeI fragment into the pEGFP-C1 vector opened with XhoI and EcoRI.

RFP tagged WT CLASP2 and CLASP2 mutants were based in the CSII-CMV-MCS lentiviral vector. CLASP2 $\gamma$  (60-1294aa) sequences were inserted between NdeI-NotI sites. CLASP mutant constructs contained the following point mutations: IP12 (I496A/ P497A/ I519A/ P520A), IP12-3eaaa (I496A/ P497A/ I519A/ P520A-W667E/ K833E/ R838A/ K839A), 1ea-IP12 (W106E/ K191A-I496A/ P497A/ I519A/ P520A), 2ea-3eaaa (W106E/ K191A-W667E/ K833E/ R838A/ K839A), WT- $\Delta$ C (truncated after TOG3 region with no mutations), IP12- $\Delta$ C (truncated after TOG2 region with I496A/ P497A/ I519A/ P520A mutations), IP12-3eaaa- $\Delta$ C (truncated after TOG3 domain with I496A/ P497A/ I519A/ P520A-W667E/ K833E/ R838A/ K839A mutations). TOG2 was truncated after the TOG2 region of WT CLASP2 with no mutations. TOG2-C is the same as TOG2 with the addition of a linker (residues 273-323 of Stu2) followed by the C-terminus of



## CLASPs promote exclusive EB plus-end localization

CLASP2 $\gamma$  (residues 1034-1294). TOG2-EMTB is the same as TOG2-C, but contains the MT binding region of Enscosin (EMTB) instead of the C-terminus of CLASP2 $\gamma$ ; EMTB was obtained by PCR from the 3xGFP-EMTB plasmid (described in (Faire et al., 1999)).

The EB protein expression constructs were based on the pET22b vector. Mouse EB3-GFP was cloned into NdeI-NotI sites of pET22b resulting in a C-terminal 6xHis-tag following the GFP. The EB1N-LZ-GFP-6xHis expression construct was made by introducing a MluI site after amino acid 139 in mouse EB1 by PCR. The leucine zipper from yeast GCN4 was then added as a MluI-BamHI fragment, followed by GFP cloned into NdeI-NotI sites of the pET22b vector.

Human CLASP2 (60-1294aa) was sub-cloned into the pET21a vector, without a stop codon, and was expressed as a C-terminal histidine-tagged protein.

### *Western blotting*

Western blotting was performed with the Protein Electrophoresis and Western Blotting System (Bio-Rad). For western blotting the following antibodies were used: a mouse actin antibody (1:1000; pan-Ab-5; Thermo Scientific), a rabbit actin antibody (1:1000, Sigma), a custom rabbit CLASP2 antibody (1:500; VU-83, previously described in (Efimov et al., 2007)), a rabbit CLASP1 antibody (1:500; Epitomics), a mouse EB1 antibody (1:500, BD Transduction), a mouse GFP antibody (1:500, Roche) and a guinea pig CLIP-170 antibody (1:1000, Synaptic Systems). LI-COR 800 or 700 secondary antibodies were used (LI-COR, IRDye) with an Odyssey Infrared Imaging System (LI-COR). Individual western blots were run for each +TIP protein analyzed; the actin blot shown is a representative blot.

### *Protein Expression and Purification*

EB3-GFP-6xHis was bacterially expressed. For purification, cells were resuspended in lysis buffer (1% NP-40, 5 mM  $\beta$ -mercaptoethanol, protease inhibitors [1 mM PMSF; 1 mM benzamidine; and 10  $\mu$ g/ml each of leupeptin, pepstatin, and chymostatin] in 1x PNI buffer) containing 1 mg/ml lysozyme. Lysate was sonicated and clarified by centrifugation at 35,000 rpm for 1 hour in a Ti 45 rotor (Beckman). About 2 ml of Ni-NTA resin was incubated with the supernatant for 1 hour at 4°C, and then washed extensively with lysis buffer lacking NP-40 and protease inhibitors. The resin was then eluted and exchanged using a PD10 column into the final buffer (10mM K-HEPES pH 7.7, 500mM KCl, 1mM DTT), aliquoted, frozen in liquid nitrogen, and stored at - 80°C.

EB1-N-LZ-GFP-6xHis was bacterially expressed. For purification, cells were lysed by sonication in binding buffer (50mM KPO<sub>4</sub> pH 7.2, 400mM NaCl, 2mM MgCl<sub>2</sub>, 2mM  $\beta$ -mercaptoethanol, 12mM imidazole) containing 0.1% Triton X-100, 1mg/ml lysozyme and 1mM PMSF. After centrifugation, the supernatant was incubated with Ni-NTA agarose, washed with binding buffer containing 20mM imidazole and eluted with 250mM imidazole. The EB1 containing fractions were loaded onto a Superdex 200 16/60 column (GE

## CLASPs promote exclusive EB plus-end localization

Healthcare) equilibrated with binding buffer lacking imidazole and eluted in the same buffer. Peak fractions were combined and concentrated using vivaspin columns (Sartorius), supplemented with 20% glycerol, aliquoted, frozen and stored in liquid nitrogen.

Tubulin was purified according to published protocols (Castoldi and Popov, 2003). Human CLASP2 (60-1294aa) was bacterially expressed as a C-terminal histidine-tagged protein. CLASP2 was purified using Ni-NTA Superflow, followed by HiTrapSP. The protein was eluted into elution buffer (20mM PIPES, 20mM MES, 120mM KCl, 2mM EGTA), aliquoted, frozen in liquid nitrogen, stored at - 80°C.

### *MBP Pull Down Assays*

In order to investigate protein-protein interactions, MBP-EB1 was used as bait to test for CLASP (WT $\Delta$ C or IP12 $\Delta$ C) binding. 50ug of MBP-EB1 was immobilized on amylose resin (NEB) then incubated with 500pmol CLASP protein for 10min at room temperature and washed 5 times with buffer containing 20mM Tris (pH 8), 0.15M NaCl, and 1mM DTT. MBP-EB1 was eluted from the resin by buffer supplemented with 10mM maltose.

### *Quantitative analysis*

For line scans, analysis of fluorescence intensity distribution of +TIPs along MTs in cells was performed using ImageJ software. The freehand line tool was used to draw a line (width of 3) along the length of the MT using  $\alpha$ -tubulin staining as a guide. The point where pixel intensity abruptly changed was considered the microtubule tip. The plot profile algorithm was used to obtain fluorescence intensity values along this line. After background subtraction, line-scans were normalized via setting the average peak intensities to 1. For appropriate conditions, the average peak intensity was not normalized to 1 in order to accurately reflect decreased tip localization due to dominant negative displacement (CLIP-170 in Figure 2I and Figure 2K) or siRNA depletion (EB1 in Figure 1K). In these situations, the experimental condition's line scan was graphed proportionally to the line scan of the control by dividing both line scans by the control peak value. Lattice to Tip ratios in cells were calculated as the average normalized intensity 2um from the start of the MT (lattice) divided by the average normalized peak intensity (tip). Line-scans were acquired at random for 5 MTs per cell from 5 cells each in 2 independent experiments (total n=50). All images were taken at the same microscope settings.

For line scans analysis of EB1N-LZ-GFP fluorescence intensity along MTs *in vitro*, kymographs were first generated from rolling ball background corrected image stacks (to include the GMPCPP seed, lattice, and tip) using an ImageJ plugin ([http://biop.epfl.ch/TOOL\\_KYMOGRAPH.html](http://biop.epfl.ch/TOOL_KYMOGRAPH.html)). From these kymographs, areas of growth were identified and average EB1 intensities were measured at the tip (line width of 3) and at the lattice (rectangular ROI); These values were then used to generate the *in vitro* lattice to tip ratios. The average intensity before the tip was subtracted as background.



## CLASPs promote exclusive EB plus-end localization

To generate binding curves for the MT-affinity analysis, the Gels tool in ImageJ was used to quantify EB3-GFP band intensity in the pellet by drawing a box of equal size around each lane. The intensity of each band was derived from the area under the resulting curves. EB levels were then normalized to the amount of total MT polymer for each reaction. The normalized pellet intensities were plotted as a function of EB3-GFP concentration. To determine the dissociation constant ( $K_d$ ), Prism (GraphPad) software was used to perform a hyperbolic fit of the data using a bimolecular binding equation,

$$Y = \frac{B_{max} \cdot X}{K_d + X}$$

with  $K_d$  being the dissociation constant (as previously described in (Zhu et al., 2009)). Analysis was performed over 2 independent experiments.

To calculate levels of various +TIP proteins, in CLASP-depletion or other experimental conditions, western blot analysis was performed. The Gels tool in ImageJ was used to quantify band intensities as described above. All +TIP protein levels were normalized to actin as a loading control. Analysis was performed over 3 independent experiments.

Quantification of total MT length as well as number of EB plus-ends was performed using the Surfaces package in Imaris, which fits filamentous structures in the cell. For total MT length, the area of MT surfaces calculated by Imaris was divided by the apparent MT width in pixels to find the sum of the MT length. For the number of plus-ends, the same software was used to fit EB3 comets. In CLASP-depleted cells, the gamma function in ImageJ was used prior to Imaris analysis to enhance EB3 at the plus-ends of MTs (rather than the lattice); these images were then analyzed as for control. Example images of Imaris fitting can be found in Figure S1C.

To calculate changes in levels of GTP-tubulin along MTs of CLASP-depleted cells, ImageJ was used to find the average fluorescent intensity of GTP-tubulin staining per cell, which was then averaged per condition. Because CLASP-depleted cells have decreased MT numbers, GTP-tubulin fluorescent intensity was normalized to account for changes in total MT length quantified by Imaris. All images were taken at the same microscope settings and analysis was performed over 2 independent experiments.

Analysis of EB1 and GTP-tubulin “speckle” distribution and binary fitting along MTs was performed using ImageJ and MatLab software. In brief, line scans for EB1 and GTP-tubulin were created and background was subtracted. All lines were 50 pixels in length (MT segment). To smooth EB1 speckles and highlight regions of similar fluorescent intensity, a Gaussian blur was applied (kernel radius of 1 pixel). This data was then transformed into a binary image using a relative threshold to the 25<sup>th</sup> percentile: values of 0 represented no speckle, while values of 1 represented an EB1 speckle or GTP-tubulin remnant. Once binary values, runs of consecutive values equal to 1 were counted as individual EB1/GTP-tubulin patches on the MT.

CLASPs promote exclusive EB plus-end localization

### *Microscopy and Image Acquisition*

For acquisition of low magnification images showing relative CLASP levels, wide-field fluorescence imaging of fixed cells was performed using a Nikon 80i microscope with a Nikon Plan Fluor 40x oil lens NA 1.3 and a CoolSnap ES CCD camera (Photometrics). For all other immunofluorescence imaging, a Leica TCS SP5 confocal laser scanning microscope with an HCX PL APO 100x oil lens NA 1.47 was used to acquire confocal stacks of fixed cells.

For the *in vitro* MT plus-end tracking assays, chambers were imaged using an Olympus TIRF system (100x NA 1.49 objective with 1.6x additional magnification) and a Hamamatsu ImageEM-1k back-illuminated EM-CCD camera under the control of xcellence software. Images were obtained every 0.5s with 200ms exposure for 100s.

Samples for platinum replica EM were processed as described previously (Svitkina, 2009). Briefly, cells were quickly rinsed with PBS, extracted with 1% Triton X-100 in PEM buffer (100mM PIPES-KOH, pH 6.9, 1mM MgCl<sub>2</sub>, and 1mM EGTA) containing 2% PEG (MW 35 kDa), 2uM unlabeled phalloidin, and 2uM paclitaxel (Sigma). After 3 quick rinses with PEM buffer, detergent-extracted cells were fixed sequentially with Glutaraldehyde, tannic acid, and uranyl acetate; they were then critical point dried, coated with platinum and carbon, transferred onto electron microscopic grids, and analyzed using JEM 1011 transmission EM (JEOL USA, Peabody, MA) operated at 100kV. Images were captured by an ORIUS 832.10W CCD camera (Gatan, Warrendale, PA) and presented in inverted contrast.

### *Image Processing*

For figure images, maximum intensity projections were made from confocal stacks. Unless otherwise indicated, all images are maximum intensity projections. Brightness and contrast were adjusted individually for each fluorescent channel and gamma settings were adjusted, when necessary, to make small structures more visible (*e.g.* +TIPs). Maximum intensity projections used for line-scan analysis and live cell movies used for FRAP analysis were unaltered.